

## Dichotomic ratchet in a two-dimensional corrugated channel

Pavol Kalinay<sup>1</sup> and František Slanina<sup>2</sup>

<sup>1</sup>*Institute of Physics, Slovak Academy of Sciences, Dúbravská cesta 9, 84511, Bratislava, Slovakia*

<sup>2</sup>*Institute of Physics, Czech Academy of Sciences, Na Slovance 2, CZ-18221, Prague, Czech Republic*



(Received 4 October 2021; accepted 29 November 2021; published 10 December 2021)

We consider a particle diffusing in a two-dimensional (2D) channel of varying width  $h(x)$ . It is driven by a force of constant magnitude  $f$  but random orientation there or back along the channel. We derive the effective generalized Fick-Jacobs equation for this system, which describes the dynamics of such a particle in the longitudinal coordinate  $x$ . Aside from the effective diffusion coefficient  $D(x)$ , our mapping also generates an additional effective potential  $-\gamma(x)$  added to the entropic potential  $-\log[h(x)]$ . It acquires an increasing or decreasing component in asymmetric periodic channels, and thus it explains appearance of the ratchet current. We study this effect on a trial example and compare the results of our true 2D theory with a commonly used effective one-dimensional description; the data are verified by the numerical solution of the full 2D problem.

DOI: [10.1103/PhysRevE.104.064115](https://doi.org/10.1103/PhysRevE.104.064115)

### I. INTRODUCTION

Rectification of the random motion of particles due to the ratchet effect is a widespread phenomenon [1,2]. It appears as a consequence of concerted effect of broken spatial reflection symmetry, nonequilibrium, and energy input from outside, which also breaks the time-reversal symmetry. The energy input can be implemented by periodic or stochastic switching of an external potential or external driving force, but it can also originate from internal structure of the particles. The latter is the case of active particles [3,4], which may be of natural or artificial origin. The paradigmatic example is the Janus particles [5,6], which are chemically propelled and change their direction randomly.

The ratchet effect with active particles was discovered experimentally using bacteria [7] and subsequently observed in numerous settings with both natural and artificial particles [8–13]. Rectification of active particles was studied theoretically by computer simulations in a two-dimensional (2D) patterned environment [14–17] as well as in quasi-one-dimensional (1D) channels of a periodically varying profile [18–22]. The common mechanism in both 2D and quasi-1D ratchets is selective trapping of particles which are propelled contrary to the “easy” direction. What the “easy” direction is in a specific case depends on the details of the geometry. The typical trapping time is the inverse of the frequency  $\alpha$  with which the direction is switched. When the frequency  $\alpha$  becomes large, the particles approach the limit of ordinary passive particles and the ratchet effect disappears. Therefore, it makes sense to consider the case of weakly active particles, where  $\alpha$  is large but finite, and to develop a kind of  $1/\alpha$  expansion. Let us remark that if the change of direction is due to rotation of the Janus particle by thermal fluctuations, the rotational diffusion coefficient, related to  $\alpha$ , depends on the inverse cube of particle diameter, while the translational diffusion is inversely proportional to it. Therefore for small

enough particles, the rotational diffusion can be by orders of magnitude faster than the spatial diffusion, and thus considering large  $\alpha$  is physically plausible.

In this work we consider a single active particle diffusing in a two-dimensional (2D) channel of varying width  $h(x)$ . Compared to the Janus particles, whose internal driving force can be oriented arbitrarily in space [5], the behavior of the particle in our model is simplified so that the internal driving force can point only along the direction of the channel axis, with a fixed magnitude  $f$  and randomly flipping sign. In fact, it is equivalent to a passive particle driven by a constant external force  $f$  acting forward or backward along the channel (see Fig. 1). Indeed, on a single-particle level there is no distinction between an active particle and passive particle in stochastically changing external field (provided we neglect the hydrodynamic details of the propulsion mechanism).

The driving force flips randomly between the two possible orientations with the rate  $\alpha$ . The mean force averaged over long time is zero, but asymmetry of the channel, given by the shaping function  $h(x)$ , causes a different response of the particle at the walls to the driving forward or backward, and so its net velocity can appear nonzero. The state of the particle is described by three degrees of freedom: longitudinal coordinate  $x$ , transverse coordinate  $y$ , and direction of the driving. However, the ratchet current flows only along the first of the three, which leads us to the idea of projecting the remaining two coordinates out using a kind of the mapping technique [23–29]. Having derived the effective reduced 1D equation of the Fick-Jacobs (FJ) type [23], one can easily apply the Stratonovich [30,31] or the Lifson-Jackson [32] formula to calculate the net current or the velocity of the particle.

The ratchet effect with active particles in 1D periodic potentials was also studied directly both analytically and with numerical simulations [33–36], and these approaches could be in principle seamlessly joined to the FJ technique. In the context of active particles, the mapping was already used in

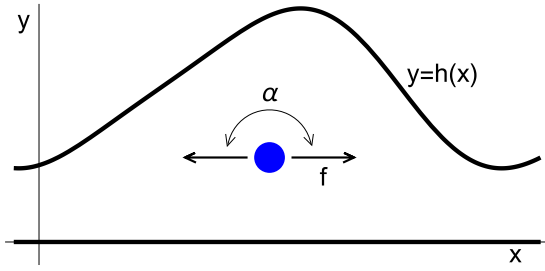


FIG. 1. Scheme of the ratchet driven by fluctuating force  $f$  in a 2D channel.

Refs. [37–39]. The models of confined particles self-propelled in an arbitrary 2D or three-dimensional (3D) direction were considered, which are rather complicated for studying the correlations between motions in the particular degrees of freedom. The spatial diffusion was reduced to the 1D problem applying the FJ approximation, either basic or modified by the Reguera-Rubí effective diffusion coefficient  $D(x)$  [40,41]. Moreover, the effect of angular diffusion was studied, which might be interpreted as investigation of 1D motion of particles with an internal degree of freedom. Of course, the translational motion of particles is influenced by random orientation of their propulsion, namely, at the curved boundary, and so the easy reduction of the spatial transverse coordinate may not work satisfactorily. In our simplified model, we present a method reducing simultaneously both degrees of freedom, the coordinate  $y$  and orientation of the flipping force  $f$ , reflecting more appropriately the correlations of motion in all directions.

The technique of dimensional reduction was developed for the diffusion alone in a 2D or 3D corrugated channel [24–26]. It is based on the scaling of the transverse diffusion constant by a factor  $1/\epsilon$ , which is equivalent to scaling of the transverse lengths by  $\sqrt{\epsilon}$ . If the scaling parameter  $\epsilon \rightarrow 0$ , the diffusion across the channel becomes infinitely fast, smearing immediately the transverse profile of the particle probability density  $\rho$  to a constant,  $\rho(x, y, t) = \rho(x, t)$ . Integration of the diffusion equation over the cross section then results in the FJ equation [23], depending on the only spatial coordinate  $x$ .

Small but nonzero  $\epsilon$  slows down the transverse relaxation, and the transverse profile of  $\rho$  begins to deflect from  $\rho(x, t)$ . The deviations can be formally expressed as a series in powers of  $\epsilon$ , depending on  $y$ , the local width of the channel  $h(x)$ , and its derivatives. After some algebra, it leads to a series of corrections to the FJ equation, expressed finally by the effective diffusion coefficient  $D(x)$ , replacing the intrinsic diffusion constant  $D_0$ . The mapping technique was later extended to diffusion in various conservative fields [27–29].

Recently a similar technique was used to derive the reduced dynamics of the 1D dichotomic ratchet [36]. Diffusion of a particle pushed forward or backward by the randomly flipping force  $f$  was studied on a line in the potential  $U(x)$ . The orientation of the flipping force was considered as the “transverse” coordinate to be reduced, and the inverse flipping rate  $1/\alpha$  played the role of the small parameter. In the limit  $\alpha \rightarrow \infty$ , the infinitely fast flipping makes the force  $f$  ineffective to the motion of particles, so the reduced 1D equation is the Smoluchowski equation in the potential  $U(x)$ .

For a finite  $\alpha$ , the particle has a time  $\sim 1/\alpha$  to move before the next flip, and thus its probability density starts to deflect from that given by the Smoluchowski equation with only  $U(x)$ . Again, the deviations can be formally expressed as a series in  $1/\alpha$ , and finally, the Smoluchowski equation is corrected by the terms depending on  $f$ ,  $\alpha$ , and the derivatives of  $U(x)$ . Aside from the effective diffusion coefficient  $D(x)$ , an additional effective potential  $-\gamma(x)$  also appears in the mapped equation. In asymmetric periodic channels, it can contain an increasing or decreasing contribution, driving effectively the ratchet current.

In the present work, we are interested in a similar model of dichotomic ratchet, where the particles diffuse in a non-homogeneous 2D channel instead of the 1D landscape  $U(x)$ . We combine here the mapping schemes of both mentioned models, reducing the transverse coordinate  $y$  as well as the orientation of the force. The result is again the generalized FJ equation, extended by the diffusion coefficient  $D(x)$  and the additional potential  $-\gamma(x)$ , which also consists of two parts in asymmetric periodic channels: a periodic one and a contribution depending linearly on  $x$ . The last one determines the appearance of the ratchet effect.

In Sec. II we formulate the problem and discuss the zeroth-order approximation, which is formally identical to the model of a particle in the 1D entropic potential  $U(x) = -\ln h(x)$  [36]. The mapping procedure for the true 2D channel is then presented in Sec. III. We demonstrate the resulting ratchet current on a trial channel and compare it with the commonly used FJ approximation. Our data are also verified by the numerical solution of the full-dimensional equations.

## II. SPATIAL FICK-JACOBS APPROXIMATION

First, we formulate here the equations to be solved. The driving of particles there or back by the flipping force  $f$  can be carried out in various ways: either the direction of an external force is flipping, or it is the Janus particle [5], self-propelled forward or backward depending on its orientation. We can consider two species of particles, pushed forward (+) or backward (−) by the force  $+f$  or  $-f$ , respectively, along the  $x$  axis. The equations governing their probability densities  $\rho_{\pm}$  are

$$\partial_t \rho_{\pm}(x, y, t) = D_0 \left[ \partial_x (\partial_x \mp f) + \frac{1}{\epsilon} \partial_y^2 \right] \rho_{\pm}(x, y, t) \mp \alpha [\rho_+(x, y, t) - \rho_-(x, y, t)], \quad (2.1)$$

describing the driven diffusion by the force  $\pm f$  and flipping between the species ( $\pm$ ) with the rate constant  $\alpha$ . We suppose the energy measured in the units such that the temperature  $k_B T = 1$ . The transverse diffusion constant is supposed  $1/\epsilon$  times larger than the longitudinal one  $D_0$ , having introduced the scaling parameter  $\epsilon$  necessary for the mapping procedure. We also divide Eq. (2.1) by  $D_0$  and scale the time  $D_0 t \rightarrow t$ , as well as the rate constant  $\alpha/D_0 \rightarrow \alpha$ . The equation is supplemented by the no-flux boundary conditions (BC) at the boundaries  $y = 0$  and  $y = h(x)$  for each orientation,

$$\begin{aligned} \partial_y \rho_{\pm}(x, y, t)|_{y=h(x)} &= \epsilon h'(x) (\partial_x \mp f) \rho_{\pm}(x, y, t)|_{y=h(x)}, \\ \partial_y \rho_{\pm}(x, y, t)|_{y=0} &= 0; \end{aligned} \quad (2.2)$$

the prime denotes the derivative according to  $x$ .

Now we reduce the spatial coordinate  $y$  by integration over the cross section. The 1D (marginal) densities

$$p_{\pm}(x, t) = \int_0^{h(x)} \rho_{\pm}(x, y, t) dy \quad (2.3)$$

have to obey Eq. (2.1) integrated over  $y$ ,

$$\begin{aligned} \partial_t p_{\pm}(x, t) &= \partial_x [(\partial_x \mp f) p_{\pm}(x, t) - h'(x) \rho_{\pm}(x, h(x), t)] \\ &\mp \alpha [p_+(x, t) - p_-(x, t)], \end{aligned} \quad (2.4)$$

obtained using the integration by parts and applying the BC (2.2). To gain the self-consistent equations for  $p_{\pm}$ , we still need to express the 2D densities  $\rho_{\pm}(x, h(x), t)$  by  $p_{\pm}(x, t)$ . In the limit  $\epsilon \rightarrow 0$ , the transverse diffusion becomes infinitely fast, smearing immediately the profiles of  $\rho_{\pm}$ ; hence  $\rho_{\pm}(x, h(x), t) = \rho_{\pm}(x, y, t) = p_{\pm}(x, t)/h(x)$ . If applied in Eq. (2.4), we arrive at the (spatial) FJ approximation

$$\begin{aligned} \partial_t p_{\pm}(x, t) &= \partial_x h(x) (\partial_x \mp f) [p_{\pm}(x, t)/h(x)] \\ &\mp \alpha [p_+(x, t) - p_-(x, t)] \end{aligned} \quad (2.5)$$

after some algebra.

Notice that this equation is equivalent to that defining the 1D model, Eq. (1.1) in Ref. [36], if we take the 1D potential as the entropic one in the 2D channel,  $U(x) = -\ln[h(x)]$ ; this approximation is often used for solving the nonhomogeneous 2D models [33,37,39]. To compare it with a more precise calculation in the next section, we review here the key results of the mapping presented in Ref. [36] with  $U(x)$  expressed by  $h(x)$ , and demonstrate them on a trial channel.

The mapped equation, reducing the orientation of  $f$ , has the form of the generalized FJ equation,

$$\partial_t p(x, t) = \partial_x h(x) e^{\gamma(x)} [1 - \hat{Z}(x, \partial_x)] \partial_x e^{-\gamma(x)} \frac{p(x, t)}{h(x)}, \quad (2.6)$$

governing the 1D density of both orientations,

$$p(x, t) = p_+(x, t) + p_-(x, t). \quad (2.7)$$

The function  $\gamma(x)$  and the operator  $\hat{Z}(x, \partial_x)$  express the corrections to the zeroth-order FJ equation,  $\partial_t p(x, t) = \partial_x h(x) \partial_x [p(x, t)/h(x)]$ . It is valid in the limit  $\alpha \rightarrow \infty$ , when the diffusing particle has no time to react to the fast flipping force and the densities  $p_{\pm}(x, t) = p(x, t)/2$ .

For a finite  $\alpha$ , the densities  $p_{\pm}$  deflect from  $p/2$  due to different responses of the particles to the driving uphill or downhill in the entropic potential  $-\ln[h(x)]$  by the force  $f$  between the succeeding flips. Expressing formally the difference  $p_+(x, t) - p_-(x, t)$  using  $p(x, t)$ , the corrections included in  $\gamma(x)$  and  $\hat{Z}(x, \partial_x)$  are determined recursively, expanded in  $1/\alpha$ ,

$$\begin{aligned} \hat{Z}(x, \partial_x) &= -\frac{f^2}{2\alpha} - \frac{f^2}{4\alpha^2} \left(\frac{h'}{h}\right)' + \frac{1}{8\alpha^3} \left\{ f^4 \partial_x^2 \right. \\ &+ \left[ \frac{3f^4 h'}{h} - \frac{2f^2}{h^3} (h^2 h^{(3)} - 3hh'h'' + 2h^3) \right] \partial_x \\ &+ \frac{3f^4 h''}{h} + \frac{f^2}{h^4} (11h^4 - 25hh^2 h'' + 8h^2 h'^2 \\ &+ 9h^2 h' h^{(3)} - 3h^3 h^{(4)}) \left. \right\} + \dots, \end{aligned} \quad (2.8)$$

$$\begin{aligned} \gamma(x) &= \left( -\frac{f^2}{2\alpha} + \frac{f^4}{4\alpha^2} - \frac{f^6}{8\alpha^3} + \dots \right) \ln h - \frac{f^2}{4\alpha^2} \left[ \left(\frac{h'}{h}\right)' \right. \\ &+ \frac{h'^2}{2h^2} \left. \right] + \frac{f^4}{8\alpha^3} \left( \frac{2h''}{h} + \frac{h'^2}{2h^2} + \int \frac{h'^3}{h^3} dx \right) \\ &- \frac{f^2}{8\alpha^3} \left[ \frac{h^{(4)}}{h} - \frac{2h'h^{(3)}}{h^2} - \frac{5h'^2}{2h^2} + \frac{6h^2 h''}{h^3} - \frac{2h^4}{h^4} \right. \\ &+ \left. \int \left( \frac{h'^5}{h^5} - \frac{h'h'^2}{h^3} \right) dx \right] + \dots, \end{aligned} \quad (2.9)$$

up to the third order, omitting writing the obvious arguments.

The form of the mapped equation (2.6) justifies existence of two basic states: the (quasi-) equilibrium, with  $p_{eq}(x) \sim h(x)e^{-\gamma(x)}$ , and the stationary flow, when the right-hand side equals  $-\partial_x J = 0$ ; hence the net flux  $J$  is constant. For solutions close to the stationary flow, Eq. (2.6) can be reduced to a simpler form

$$\partial_t p(x, t) = \partial_x h(x) e^{\gamma(x)} D(x) \partial_x e^{-\gamma(x)} \frac{p(x, t)}{h(x)}, \quad (2.10)$$

where the operator  $\hat{Z}$  is replaced by just a function, the effective diffusion coefficient  $D(x)$ . Equations (2.6) and (2.10) represent the mass conservation of the same system, so if  $\partial_x e^{-\gamma(x)} p_{st}(x)/h(x)$  for the stationary solution  $p_{st}(x)$  is expressed from both of them and compared [25], we arrive at the relation

$$\frac{1}{D(x)} = h(x) e^{\gamma(x)} [1 - \hat{Z}(x, \partial_x)]^{-1} \frac{e^{-\gamma(x)}}{h(x)}, \quad (2.11)$$

enabling us to derive  $D(x)$  from the known  $\hat{Z}$ . Taking Eq. (2.8), we find

$$\begin{aligned} \frac{1}{D(x)} &= 1 - \frac{f^2}{2\alpha} + \frac{f^4}{4\alpha^2} - \frac{f^6}{8\alpha^3} + \dots - \frac{f^2}{4\alpha^2} \left(\frac{h'}{h}\right)' \\ &+ \frac{f^2}{8\alpha^3 h^4} (15h^4 - 31hh^2 h'' + 8h^2 h'^2 + 11h^2 h' h^{(3)}) \\ &- 3h^3 h^{(4)} + \frac{f^4}{8\alpha^3 h^2} (4hh'' - 3h'^2) + \dots \end{aligned} \quad (2.12)$$

up to the third order. The terms independent of  $h$  give  $D(x) \simeq 1 + f^2/2\alpha$ , known as the generalized Taylor dispersion correction [42,43].

Unlike the auxiliary dimensionless parameter  $\epsilon$  used in the reduction of the transverse coordinate  $y$ , the functions  $\gamma(x)$  and  $1/D(x)$  here are expanded in the meaningful quantity  $1/\alpha$  (i.e., the ratio  $D_0/\alpha$  in the unscaled time), having the dimension  $m^2$  (meters squared). Dimension of the force  $f$  measured in units with  $k_B T = 1$  is  $m^{-1}$ , so its inverse could serve as the typical length scale, forming the dimensionless small parameter  $f^2/\alpha$ , controlling convergence of the expansion. However, the terms depending on derivatives of  $h(x)$  in Eq. (2.12) violate this structure; the typical length is also given by the shape of the channel. Below we demonstrate the convergence of the results on a specific example.

Equation (2.10) has the form of 1D Smoluchowski equation with the spatial dependent diffusion coefficient; hence we can interpret the function  $-\gamma(x)$  as an additional effective potential appearing due to reduction of orientation of the flipping force  $f$ . Let us notice the integral terms  $\sim 1/\alpha^3$  in Eq. (2.9).

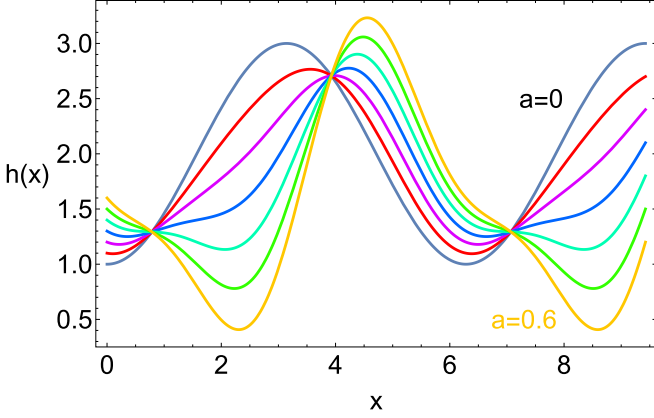


FIG. 2. Trial shaping function  $h(x)$  (2.14) for various parameters  $a = 0, 0.1, \dots$  up to 0.6.

As we show below, they can give a nonzero increment of  $\gamma(x)$  over one period  $L$  in asymmetric periodic channels,  $h(x+L) = h(x)$ . The full effective potential  $-\ln[h(x)] - \gamma(x)$  becomes a slanted washboard function, determining the effective force averaged over one period,  $\Delta\gamma/L = [\gamma(L) - \gamma(0)]/L$ , effectively driving the ratchet effect. For calculation of the stationary current in the washboard potential, we can use the Stratonovich [30,31] or the Lifson-Jackson [32] formulas,

$$J = (1 - e^{-\Delta\gamma}) \left[ \int_0^L h(x) e^{\gamma(x)} dx \int_x^{L+x} \frac{e^{-\gamma(x')}}{h(x') D(x')} dx' \right]^{-1} \simeq \Delta\gamma \left[ \int_0^L h(x) e^{\gamma(x)} dx \int_0^L \frac{e^{-\gamma(x)}}{h(x) D(x)} dx \right]^{-1} \quad (2.13)$$

(valid for small  $\Delta\gamma$ ), modified for the varying diffusion coefficient  $D(x)$ ; one particle per period  $L$  is considered. We check the presented theory on a trial shaping function

$$h(x) = (2 - \cos x)(1 + a \cos x - a \sin x), \quad (2.14)$$

enabling us to calculate the necessary integrals in Eq. (2.9) analytically. The parameter  $a$  controls anisotropy of the channel; see Fig. 2.

The corresponding ratchet current  $J$  divided by  $f^2$  for easier comparison for various  $f$  is plotted in Fig. 3, depending on  $\alpha$ . The solid and dashed lines depict the results of Eq. (2.13) for  $f = 1$  and 0.1, respectively, with  $\gamma(x)$  and  $D(x)$  derived up to the third order [Eqs. (2.9) and (2.12);  $D_0 = 1$ ]. They are compared with the stationary currents (disks and squares for  $f = 1$  and 0.1), calculated by numerical solution of Eq. (2.1). The lines represent the asymptotic  $\sim 1/\alpha^3$ , slowly approaching the exact data; let us stress that it is the lowest order in  $1/\alpha$ , exhibiting the terms resulting in nonzero  $\Delta\gamma$ . A better coincidence with the numerical data for larger  $\alpha$  can be achieved by taking the higher-order corrections to  $\gamma(x)$ ; the dotted lines show the current after adding the terms  $\sim f^2/\alpha^4$  and  $f^2/\alpha^5$  according to Eqs. (A.9) in Ref. [36] for  $f = 0.1$ . For smaller  $\alpha$  ( $< 5$  roughly here), the expansion in  $1/\alpha$  does not converge and alternative mapping methods calculating  $\gamma(x)$  and  $D(x)$  were developed [36].

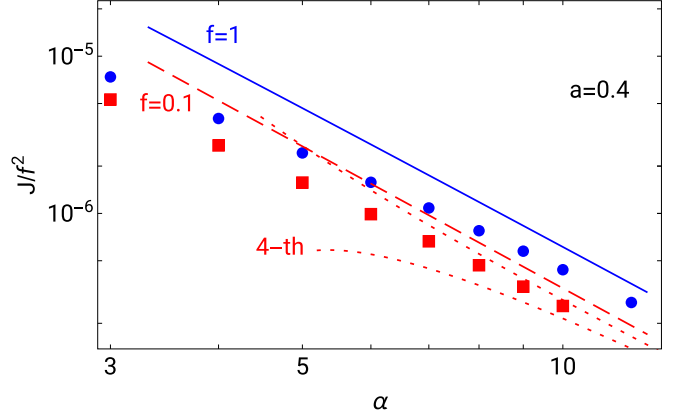


FIG. 3. The ratchet current  $J$  over  $f^2$  vs the flipping rate  $\alpha$  in the channel shaped by Eq. (2.14),  $a = 0.4$ . The blue disks and red squares correspond to the numerical solutions of Eq. (2.5) for  $f = 1$  and  $f = 0.1$ , respectively. The solid and the dashed lines represent the leading terms  $\sim 1/\alpha^3$  for  $f = 1$  and 0.1. The dotted lines demonstrate adding the 4-th-order terms  $\sim \alpha^{-4}$  and  $\sim \alpha^{-5}$  for  $f = 0.1$ .

### III. MAPPING IN 2D CHANNELS

Now we extend the mapping of Eq. (2.1) onto the longitudinal coordinate beyond the spatial FJ approximation, i.e., in the true 2D channel. To reduce both degrees of freedom, the transverse coordinate  $y$  as well as the orientation of the flipping force, we also rescale the flipping rate by  $\epsilon$ ,  $\alpha = \bar{\alpha}/\epsilon$  in Eqs. (2.1) and (2.4). The 1D density  $p(x, t)$  of our interest, Eq. (2.7), includes both orientations, so to find the corresponding mapped equation for it, we need yet to sum Eq. (2.5) over the indices  $(+)$  and  $(-)$ ,

$$\partial_t p(x, t) = \partial_x ((\partial_x - f)p_+(x, t) + (\partial_x + f)p_-(x, t) - h'(x) \times \{\rho_+[x, h(x), t] + \rho_-[x, h(x), t]\}). \quad (3.1)$$

Again, we need to express  $\rho_{\pm}(x, y, t)$  and  $p_{\pm}(x, t)$  using the 1D density  $p(x, t)$  to make Eq. (3.1) consistent. Fixing  $\bar{\alpha}$  nonzero, the parameter  $\epsilon \rightarrow 0$  makes both the transverse diffusion constant as well as the flipping rate  $\alpha$  infinite, smearing immediately the transverse profile of the density to  $\rho_+(x, y, t) = \rho_-(x, y, t) = p(x, t)/[2h(x)]$  and  $p_{\pm}(x, t) = p(x, t)/2$ . Substituting it in Eq. (3.1), we obtain the FJ equation.

A small  $\epsilon > 0$  causes a slower transverse relaxation, as well as flipping of the force. The transverse profiles of  $\rho_{\pm}(x, y, t)$  begin to deflect from  $p/2h$  in the same way as for diffusion alone [24], but also the finite flipping rate allows the  $(+)$  and  $(-)$  particles to move differently at the boundaries depending on their curvature, i.e., on  $h(x)$ . So  $\rho_+$  and  $\rho_-$  differ from one another at the boundary and also inside the channel, due to diffusion. We can express these deviations formally by operators  $\hat{w}_{\pm}(x, y, \partial_x)$  acting on  $p(x, t)$ , writing

$$\rho_{\pm}(x, y, t) = e^{\gamma(x)} \left[ \frac{1}{2} + \hat{w}_{\pm}(x, y, \partial_x) \right] e^{-\gamma(x)} \frac{p(x, t)}{h(x)}. \quad (3.2)$$

Without loss of generality, we added here the exponentials of a gauge function  $\gamma(x)$ , similar to the mapping of diffusion in a nonconservative field [44] or other studied ratchet systems [36,45]. It enables us to derive the mapped equation in the



form of generalized FJ equation (2.6). Using the formula (3.2) in Eq. (3.1) we derive

$$\partial_t p(x, t) = \partial_x e^{\gamma(x)} h(x) \left[ \partial_x + \gamma'(x) - \frac{h'(x)}{h(x)} \hat{\omega}(x, h(x), \partial_x) - \frac{f}{h(x)} \int_0^{h(x)} dy \hat{\sigma}(x, y, \partial_x) \right] e^{-\gamma(x)} \frac{p(x, t)}{h(x)} \quad (3.3)$$

after some algebra; we denoted here  $\hat{\omega} = \hat{\omega}_+ + \hat{\omega}_-$  and  $\hat{\sigma} = \hat{\omega}_+ - \hat{\omega}_-$ . The integration (2.3) and (2.7) of the backward mapped density  $\rho_{\pm}$  (3.2) has to give an identity for any  $p(x, t)$ , which also requires us to satisfy

$$\int_0^{h(x)} dy [\hat{\omega}_+(x, y, \partial_x) + \hat{\omega}_-(x, y, \partial_x)] = 0. \quad (3.4)$$

Equation (3.3) can already be transformed to the form of (2.6), having the function  $\gamma(x)$  properly fixed. As we show later, the operators  $\hat{\omega}_{\pm}(x, y, \partial_x)$  consist of the parts  $\omega_{\pm}(x, y)$ , which are just some functions, and the rest of the operators containing  $\partial_x$ ,

$$\hat{\omega}_{\pm}(x, y, \partial_x) = \omega_{\pm}(x, y) + \tilde{\omega}_{\pm}(x, y, \partial_x) \partial_x; \quad (3.5)$$

we split the operators  $\hat{\omega}$  and  $\hat{\sigma}$  in the same way. To obtain Eq. (2.6), the functional parts  $\omega_{\pm}(x, y)$  have to be eliminated by  $\gamma(x)$ ,

$$\gamma'(x) = \frac{h'(x)}{h(x)} \omega[x, h(x)] + \frac{f}{h(x)} \int_0^{h(x)} dy \sigma(x, y), \quad (3.6)$$

and then the operator  $\hat{Z}$  of Eq. (2.6) can be identified as

$$\hat{Z}(x, \partial_x) = \frac{h'(x)}{h(x)} \tilde{\omega}[x, h(x), \partial_x] + \frac{f}{h(x)} \int_0^{h(x)} dy \tilde{\sigma}(x, y, \partial_x). \quad (3.7)$$

The heart of the mapping method is derivation of the operators  $\hat{\omega}_{\pm}(x, y, \partial_x)$  and the related  $\gamma(x)$  and  $\hat{Z}(x, \partial_x)$  by the homogenization procedure. The small parameter  $\epsilon$  controls the rate of transverse equilibration, as well as the frequency of flipping, and thus the deviations of  $\rho_{\pm}$  from  $p/2h$  too. So we expect any operator or function  $F$  (denoting  $\hat{\omega}$ ,  $\hat{Z}$ , or  $\gamma$ ) expanded in  $\epsilon$ ,

$$F(\cdot) = \sum_{n=1}^{\infty} \epsilon^n F_n(\cdot). \quad (3.8)$$

We require the backward mapped density  $\rho_{\pm}(x, y, t)$ , Eq. (3.2), to satisfy the original 2D problem. So we substitute it in Eq. (2.1),

$$0 = \left( \frac{1}{2} + \hat{\omega}_{\pm} \right) \frac{e^{-\gamma}}{h} \partial_t p - \frac{1}{\epsilon} [\partial_y^2 \hat{\omega}_{\pm} \mp \bar{\alpha}(\hat{\omega}_+ - \hat{\omega}_-)] e^{-\gamma} \frac{p}{h} - e^{-\gamma} \partial_x (\partial_x \mp f) e^{\gamma} \left( \frac{1}{2} + \hat{\omega}_{\pm} \right) e^{-\gamma} \frac{p}{h}, \quad (3.9)$$

as well as in the BC (2.2),

$$0 = [\partial_y - \epsilon h' e^{-\gamma} (\partial_x \mp f) e^{\gamma}] \left( \frac{1}{2} + \hat{\omega}_{\pm} \right) e^{-\gamma} \frac{p}{h} \Big|_{y=h(x)},$$

$$0 = \hat{\omega}_{\pm} e^{-\gamma} \frac{p}{h} \Big|_{y=0}. \quad (3.10)$$

The time derivative in Eq. (3.9) commuted with all spatial operators and finally for  $\partial_t p(x, t)$ , the mapped equation (2.6)

is taken. We arrive at the equations, which have to be satisfied for any 1D solution  $p$ , or  $e^{-\gamma} p/h$  on the level of operators, fixing recursively  $\hat{\omega}_{\pm}$ .

It is convenient to write directly the operator equations for  $\hat{\omega}$  and  $\hat{\sigma}$ , necessary in the relations (3.6) and (3.7). Expressing the terms  $\sim 1/\epsilon$  from Eq. (3.9) and adding or subtracting them for the opposite indices, we find

$$\begin{aligned} \frac{1}{\epsilon} \partial_y^2 \hat{\omega} &= (1 + \hat{\omega}) \frac{1}{h} (\partial_x + \gamma') h (1 - \hat{Z}) \partial_x \\ &\quad - (\partial_x + \gamma') [(\partial_x + \gamma') (1 + \hat{\omega}) - f \hat{\sigma}], \\ \frac{1}{\epsilon} [\partial_y^2 - 2\bar{\alpha}] \hat{\sigma} &= \hat{\sigma} \frac{1}{h} (\partial_x + \gamma') h (1 - \hat{Z}) \partial_x \\ &\quad - (\partial_x + \gamma') [(\partial_x + \gamma') \hat{\sigma} - f(1 + \hat{\omega})], \end{aligned} \quad (3.11)$$

acting on any function of  $x$ . From BC (3.10), we get

$$\begin{aligned} 0 &= \{\partial_y \hat{\omega} - \epsilon h' [(\partial_x + \gamma') (1 + \hat{\omega}) - f \hat{\sigma}]\}_{y=h(x)}, \\ 0 &= \{\partial_y \hat{\sigma} - \epsilon h' [(\partial_x + \gamma') \hat{\sigma} - f(1 + \hat{\omega})]\}_{y=h(x)}, \\ 0 &= \partial_y \hat{\omega}|_{y=0} = \partial_y \hat{\sigma}|_{y=0}. \end{aligned} \quad (3.12)$$

Now, applying the expansions of  $\hat{\omega}$ ,  $\hat{\sigma}$ , and  $\gamma$  in  $\epsilon$ , Eq. (3.8), and collecting the terms of the same powers of  $\epsilon$  in Eq. (3.11), we obtain the recurrence relations determining the coefficients  $\hat{\omega}_n$  and  $\hat{\sigma}_n$ . Finding the right-hand sides, we need to solve easy ordinary differential equations in  $y$ ,  $\partial_y^2 \hat{\omega}_n = \hat{R}_n$ , and  $[\partial_y^2 - 2\bar{\alpha}] \hat{\sigma}_n = \hat{S}_n$ . Solving the second one by the variations of constants, we get

$$\begin{aligned} \hat{\sigma}_n &= e^{\sqrt{2\bar{\alpha}}y} \left( \int \frac{dy}{2\sqrt{2\bar{\alpha}}} e^{-\sqrt{2\bar{\alpha}}y} \hat{S}_n + \hat{C}_+ \right) \\ &\quad - e^{-\sqrt{2\bar{\alpha}}y} \left( \int \frac{dy}{2\sqrt{2\bar{\alpha}}} e^{\sqrt{2\bar{\alpha}}y} \hat{S}_n + \hat{C}_- \right). \end{aligned} \quad (3.13)$$

The integration constants  $\hat{C}_{\pm}(x, \partial_x)$  are fixed to satisfy the corresponding orders of  $\epsilon$  in the BC (3.12) and Eq. (3.4). Having  $\hat{\omega}_n$  and  $\hat{\sigma}_n$  expressed, the coefficients  $\gamma'_n$  and  $\hat{Z}_n$  are obtained from Eqs. (3.6) and (3.7).

We demonstrate the recurrence procedure on calculation of the first-order corrections in detail. To derive the equations for  $\hat{\omega}_1$  and  $\hat{\sigma}_1$ , we have to collect the terms  $\sim \epsilon^0$  in Eqs. (3.11),

$$\begin{aligned} \partial_y^2 \hat{\omega}_1 &= \frac{1}{h} \partial_x h \partial_x - \partial_x^2 = \frac{h'}{h} \partial_x, \\ [\partial_y^2 - 2\bar{\alpha}] \hat{\sigma}_1 &= f \partial_x; \end{aligned} \quad (3.14)$$

$\hat{\omega}$ ,  $\hat{\sigma}$ ,  $\gamma'$ , and  $\hat{Z}$  on the right-hand side are  $\sim \epsilon$ , and thus they do not contribute. The solutions

$$\begin{aligned} \hat{\omega}_1 &= \left( \frac{y^2}{2} - \frac{h^2}{6} \right) \frac{h'}{h} \partial_x, \\ \hat{\sigma}_1 &= -\frac{f h' \sinh(\sqrt{2\bar{\alpha}}y)}{\sqrt{2\bar{\alpha}} \cosh(\sqrt{2\bar{\alpha}}h)} - \frac{f}{2\bar{\alpha}} \partial_x \end{aligned} \quad (3.15)$$

satisfy  $\partial_y \hat{\omega}_1 = \partial_y \hat{\sigma}_1 = 0$  at  $y = 0$  and  $\partial_y \hat{\sigma}_1 = -f h'$  at  $y = h(x)$  from the BC (3.12), which are required in any order of  $\epsilon$ . The second integration constant of  $\hat{\omega}_1$  is held by the condition of consistency, Eq. (3.4), in the order  $\sim \epsilon^1$ . The BC for  $\hat{\omega}_n$  at  $y = h(x)$  becomes an identity.

Now we apply  $\hat{\omega}_1$  and  $\hat{\sigma}_1$  in Eqs. (3.6) and (3.7) to find  $\gamma'_1$  and  $\hat{Z}_1$ . The operator  $\hat{\sigma}_1$  is apparently of the form  $\sigma_1(x, y) + \tilde{\sigma}_1 \partial_x$ , while  $\hat{\omega}_1$  contains only the  $\tilde{\omega}_1$  part, so

$$\begin{aligned}\hat{Z}_1 &= \frac{h'^2}{3} - \frac{f^2}{2\bar{\alpha}}, \\ \gamma'_1 &= -\frac{f^2 h'}{2\bar{\alpha} h}.\end{aligned}\quad (3.16)$$

We can easily identify the first term in  $\hat{Z}_1$  as the Zwanzig-Reguera-Rubí [40,41] leading correction to the effective diffusion coefficient due to varying width of the channel. The other contributions are identical with the first-order terms  $\sim f^2/\alpha$  in Eqs. (2.8) and (2.9).

Complexity of the results quickly grows in the higher orders; the terms  $\sim \epsilon^1$  in Eqs. (3.11) give the equations defining  $\hat{\omega}_2$  and  $\hat{\sigma}_2$ ,

$$\begin{aligned}\partial_y^2 \hat{\omega}_2 &= \hat{\omega}_1 \left( \partial_x + \frac{h'}{h} \right) \partial_x - \left( \partial_x + \frac{h'}{h} \right) \hat{Z}_1 \partial_x \\ &\quad - \partial_x \gamma'_1 - \partial_x^2 \hat{\omega}_1 + \partial_x f \hat{\sigma}_1, \\ [\partial_y^2 - 2\bar{\alpha}] \hat{\sigma}_2 &= \hat{\sigma}_1 \left( \partial_x + \frac{h'}{h} \right) \partial_x + \gamma'_1 f - \partial_x^2 \hat{\sigma}_1 \\ &\quad + \partial_x f \hat{\omega}_1.\end{aligned}\quad (3.17)$$

Solving them with the terms of BC (3.12) and Eq. (3.4)  $\sim \epsilon^2$  and finally applying the results in Eqs. (3.6) and (3.7), we obtain

$$\begin{aligned}\hat{Z}_2 &= \frac{2hh'}{45} (hh')' \partial_x + \frac{h'}{45} (h^2 h^{(3)} + hh'h'' - 7h'^3) \\ &\quad + \frac{f^2}{4\bar{\alpha}^2} \left[ \frac{4}{3} \bar{\alpha} h'^2 - \left( \frac{h'}{h} \right)' \right], \\ \gamma'_2 &= \frac{f^2}{4\bar{\alpha}^2} \left[ \frac{f^2 h'}{h} - \frac{h^{(3)}}{h} + \frac{h' h''}{h^2} \left( 1 + \kappa \coth \kappa + \frac{\kappa^2}{3} \right) \right. \\ &\quad \left. - \frac{h'^3}{h^3} \left( \kappa \coth \kappa - \frac{2\kappa^2}{3} \right) \right],\end{aligned}\quad (3.18)$$

abbreviating  $\kappa = \sqrt{2\bar{\alpha}}h(x)$ . Again, we can recognize the second-order correction for diffusion alone in  $\hat{Z}_2$ ; see Eq. (8) in Ref. [24], as well as the  $\alpha^{-2}$  term in Eq. (2.8) due to the flipping force. If we return back to the unscaled flipping rate  $\alpha = \bar{\alpha}/\epsilon$ ,  $\kappa$  becomes proportional to  $\sqrt{\epsilon}$ . Expressing then the limit of  $\gamma'_2$ , Eq. (3.18), for  $\epsilon \rightarrow 0$ , we recover correctly the coefficient  $\sim 1/\alpha^2$  of the derivative of Eq. (2.9). Let us notice that unlike the spatial FJ approximation (2.9), the integration of  $\gamma'_2$  here cannot be completed analytically for an arbitrary  $h(x)$ . So we can expect that  $\Delta\gamma$  can also be nonzero in a lower order than  $\sim 1/\alpha^3$  for  $\epsilon > 0$  in periodic asymmetric channels.

Having the mapped equation of the form (2.6), we can replace the operator  $\hat{Z}$  by the effective diffusion coefficient  $D(x)$  in the limit of stationary flow. Adopting the argumentation in Sec. II, we use formula (2.11), obtaining

$$\begin{aligned}\frac{1}{D(x)} &= 1 + \epsilon \left( \frac{h'^2}{3} - \frac{f^2}{2\bar{\alpha}} \right) + \epsilon^2 \left\{ \frac{h'}{45} [h^2 h^{(3)} - hh'h''] \right. \\ &\quad \left. - 4h'^3 \right] + \frac{f^2}{4\bar{\alpha}^2} [f^2 - (h'/h)'] \Big\} + \dots\end{aligned}\quad (3.19)$$

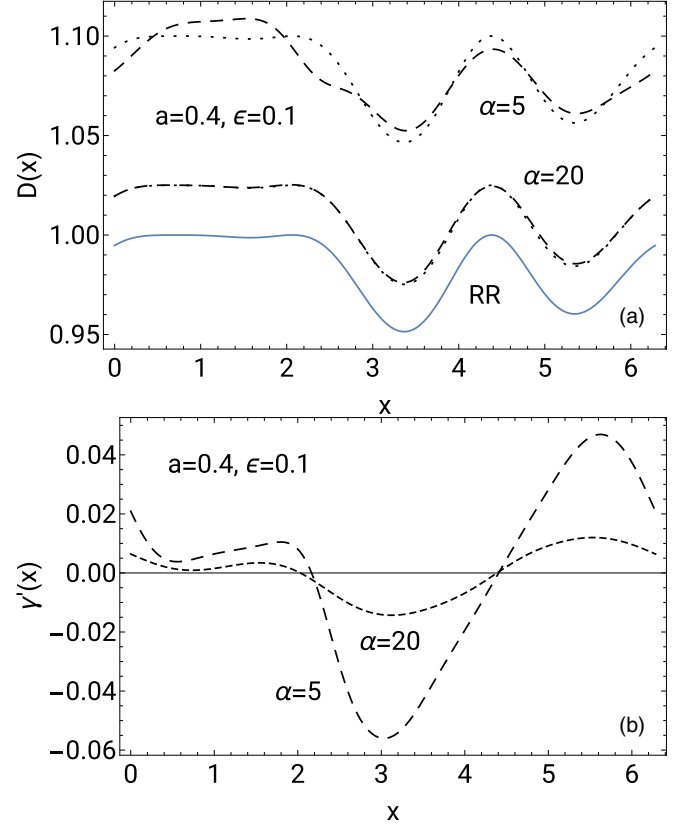


FIG. 4. The effective diffusion coefficient  $D(x)$  (a) and the local effective force  $\gamma'(x)$  (b) calculated for the channel shaped by Eq. (2.14) with  $a = 0.4$ ,  $\epsilon = 0.1$ , and  $\alpha = 5$  (long dashes) or 20 (short dashes). RR in (a) represents the corresponding Reguera-Rubí formula for diffusion alone; dotted lines depict Eq. (3.21).

up to the second order. The third-order corrections to  $\gamma'(x)$  and  $1/D(x)$  are given in the Appendix. Substituting backward  $\bar{\alpha} = \epsilon\alpha$  in Eq. (3.19) and the formulas for  $\gamma'_n(x)$  of any order  $n$ , the limit  $\epsilon \rightarrow 0$  at a fixed finite  $\alpha$  recovers the expansions of  $1/D(x)$  and  $\gamma'(x)$  in  $1/\alpha$  of the 1D model, Eq. (2.12), and the derivative of (2.9).

We demonstrate the effective diffusion coefficient  $D(x)$  and the effective local force  $\gamma'(x)$ , calculated up to the  $\sim \epsilon^3$  order, for  $h(x)$  defined by the function (2.14) in Fig. 4. The dashed lines representing  $D(x)$  for  $\alpha = 5$  and 20 are compared with the Reguera-Rubí formula [25,41],

$$D(x) \simeq \frac{\arctan[\sqrt{\epsilon}h'(x)]}{\sqrt{\epsilon}h'(x)} \simeq [1 + \epsilon h^2(x)]^{-1/3}, \quad (3.20)$$

which is the leading correction of the FJ equation for the diffusion alone. In the presence of the flipping force, this function is raised roughly by the generalized Taylor dispersion term  $f^2/2\alpha$  [42,43] of the 1D reduced model, Eq. (2.12), in the spirit as suggested by Sandoval and Dagdug [37],

$$D(x) \simeq \frac{1 + f^2/2\alpha}{[1 + \epsilon h^2(x)]^{1/3}} \quad (3.21)$$

(dotted lines), at least in the range of parameters (small  $\epsilon$  and large  $\alpha$ ) studied in this paper. The effective force  $\gamma'(x)$  varies around zero with the integral  $\Delta\gamma = 0.000895$  and  $0.000301$

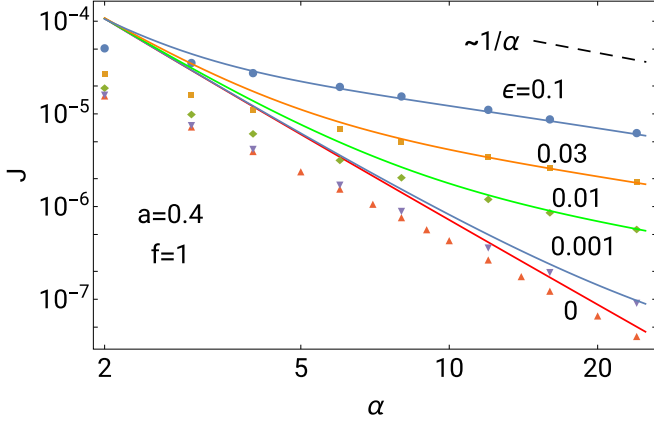


FIG. 5. The rectified current  $J$  in a channel defined by Eq. (2.14),  $a = 0.4$ , depending on the flipping rate  $\alpha$  of the force  $f = 1$ , for various inverse transverse diffusion coefficients  $\epsilon$ . The solid lines represent our theory with the formulas for  $\gamma'(x)$  and  $D(x)$  derived up to the third order. The symbols depict the results of numerical solutions of the full 2D model. The dashed line shows  $1/\alpha$  dependence.

over one period for  $\alpha = 5$  and 20, which is much smaller than the amplitude of variations. Behavior of these functions enables us to apply the simpler Lifson-Jackson formula (2.13) for calculation of the rectified current.

The rectified current  $J$  normalized to one particle per period  $L$  in a channel shaped by Eq. (2.14), depending on  $\alpha$ , is shown in Fig. 5. The solid lines were calculated according to the formulas for  $D(x)$  and  $\gamma'(x)$  derived up to the order  $\sim \epsilon^3$  for various parameters  $\epsilon$ . The line for  $\epsilon = 0$  is identical to the result of the 1D (spatial FJ) model, Eqs. (2.9) and (2.12), also taking only the leading term  $\sim 1/\alpha^3$  into account. With growing  $\epsilon$ , the decreasing speed of the transverse relaxation causes deflection of the corresponding lines from the 1D asymptotic for larger  $\alpha$ , where the current  $J$  decreases roughly  $\sim 1/\alpha$ .

We observe that slower transverse relaxation ( $\sim 1/\epsilon$ ) results in a larger rectified current. We explain it in Fig. 6, depicting the 2D density  $\rho = \rho_+ + \rho_-$  and the streamlines in the asymmetric channel shaped by Eq. (2.14),  $a = 0.2$ , for  $\epsilon = 0.3$  (a) and 0.03 (b) (see the Appendix for details of this calculation). The motor driving the circulating currents works at the curved boundary, where the particles pushed against the wall increase their density towards the bottlenecks. The variations of density at the boundary are transmitted to the bulk by diffusion alone. But the rectification mechanism does not work there; the mean velocity due to driving by the flipping force in the bulk is zero. So the particles diffuse back to the boundary at the place of the lowest density, near the maximum  $h(x)$ . Due to asymmetry of the channel, the left and right circulating currents are not symmetric, so periodicity of the density requires leaking of the rectified current between the neighboring whirls along the channel. Smaller  $\epsilon$  (panel b) causes faster transverse diffusion; the particles get quickly out of the boundary, and the rectification mechanism works worse; the net current  $J$  is smaller, as seen in Fig. 5.

The results of the mapping are checked by the numerical solution of the full 2D problem, depicted by symbols in Fig. 5. The lowest series of triangles, corresponding to  $\epsilon = 0$ , was obtained by numerical solution of the stationary 1D model;

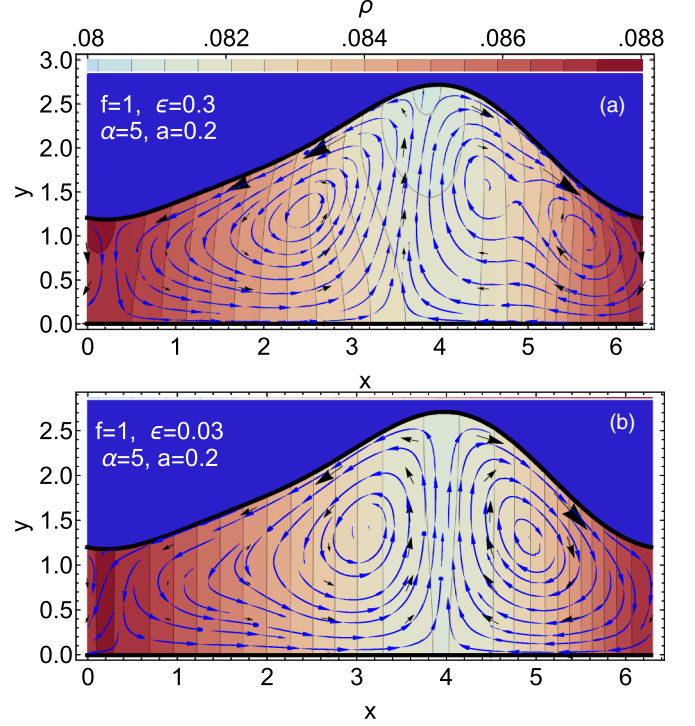


FIG. 6. Stationary 2D density  $\rho(x, y)$  (color scale) and the fluxes (streamlines) in the channel with  $a = 0.2$  for  $\epsilon = 0.3$  (a) and 0.03 (b). Size of the black arrows depicts magnitude of the flow density at the chosen positions. The rectified current flows to the left with magnitudes  $J = 5.1 \times 10^{-5}$  (a) and  $1.2 \times 10^{-5}$  (b) for one particle per period  $L = 2\pi$ .

for nonzero  $\epsilon$ , we solved numerically the full 2D problem, with the transverse diffusion coefficient enhanced by factor  $1/\epsilon$  (see the Appendix for some details of the procedure). The results for  $\epsilon = 0$  deflect visibly from the line obtained by the mapping; let us recall that the red line represents only the lowest order asymptotic  $\sim 1/\alpha^3$ . Better results can be obtained by adding the higher order contributions as analyzed in Sec. II. Surprisingly, for  $\epsilon > 0$ , much better agreement is achieved in the region where the descent of the lines approaches  $\sim 1/\alpha$ . However, our theory remains usable only for larger  $\alpha$  ( $> 5$ ). Rescaling  $\alpha$  by  $\epsilon$  in our procedure causes that the obtained expansion in  $\epsilon$  is of the same sort as the expansion in  $1/\alpha$  in the 1D case, just corrected by the finite spatial transverse relaxation. Involving also the region of smaller  $\alpha$  requires us to perform an expansion in a different parameter or a different scaling, as is indicated in Ref. [36].

#### IV. CONCLUSION

We demonstrated how to derive the effective 1D equation for a particle diffusing in a 2D channel of varying width  $h(x)$ , which is also driven along the channel there or back by the random force  $f$  flipping with the rate  $\alpha$ . The method combines the access used in the mapping of two simpler models studied before, diffusion alone in a 2D nonhomogeneous channel [24,25] and the 1D dichotomic ratchet in an (entropic) potential  $U(x) = -\log[h(x)]$  [36]. The key is to define the small parameter  $\epsilon$ , which scales both the transverse diffusion

constant as well as the flipping rate  $\alpha$ . Then we start with the same zeroth-order approximation, the FJ equation, which is valid for both particular models in the limit of infinitely fast relaxation in the (spatial) transverse direction or the flipping rate.

Then the mapping procedure generates recursively the corrections to the FJ equation, which are involved in the operator  $\hat{Z}$ , the effective diffusion coefficient  $D(x)$ , and the function  $\gamma(x)$  in Eq. (2.6) or (2.10) in the limit of the stationary flow. For the appearance of the ratchet effect, it is important to know especially  $-\gamma(x)$ , representing the additional effective potential due to the flipping force. Its structure shows that its increment  $\Delta\gamma$  over one period  $L$  for a periodic asymmetric channel can be nonzero, so  $\Delta\gamma/L$  is an effective force driving the ratchet current  $J$ . In the 1D model, such terms appear in the third order, hence the asymptotic of  $J \sim 1/\alpha^3$ . The function  $\gamma(x)$  for the true 2D channel is more complicated, enhanced by the terms depending on the finite diffusion rate across the channel for  $\epsilon > 0$ ; so the terms giving the nonzero  $\Delta\gamma$  also appear in lower orders.

We tested our theory on the periodic asymmetric channel shaped by the function (2.14). For  $\epsilon > 0$ , the rectified current  $J$  depending on  $\alpha$ , Fig. 5, deflects from the 1D asymptotic  $\sim 1/\alpha^3$  for sufficiently large  $\alpha$ . The current exhibits there rather  $\sim 1/\alpha$  decay, and its values are much larger than those for the 1D model. It is necessary to stress that the mechanism of rectification in 2D channels differs noticeably from that in the 1D potential. The rectified current appears here as a result of different motion of the particles driven there or back at the curved boundaries. There is no rectification of a particle's velocity in the bulk due to symmetry of the flipping force. Fast transverse diffusion gets the particles quickly away from the boundary to the bulk, so the ratchet effect is weaker for smaller  $\epsilon$ . The difference between the currents in the real 2D channel and in the corresponding 1D (FJ) approximation can be enormous, as is seen in Fig. 5. It is an example of a situation where a simplistic replacement of the real geometry by a 1D entropic potential is far from being satisfactory, and it is necessary to go to higher orders in the  $\epsilon$ -expansion, as we do in this work.

Scaling of the flipping rate  $\alpha$  by  $1/\epsilon$  leads to a similar type of expansions as in the 1D model, where the control parameter was  $1/\alpha$ . So validity of our results is restricted to the large flipping rates ( $\alpha > 5$ ), which was verified by comparison with the numerical solution of the full-dimensional problem. Extension of the formulas for  $D(x)$  and  $\gamma(x)$  to the region of small  $\alpha$  would require finding another small expansion parameter or, alternatively, formulate differential equations for these functions, in a way applied, e.g., in Ref. [36]. This task is left for the future.

#### ACKNOWLEDGMENT

Support from VEGA Grant No. 2/0044/21 is gratefully acknowledged.

#### APPENDIX: COMPUTATIONAL DETAILS

We give here the third-order formulas for  $1/D(x)$  and  $\gamma'(x)$ , which were used in our calculations in Sec. III but are

too complicated to be in the main text:

$$\begin{aligned} \left[ \frac{1}{D(x)} \right]_3 = & -\frac{f^6}{8\bar{\alpha}^3} + \frac{f^4}{8\bar{\alpha}^3} \left[ \frac{4h''}{h} - \frac{h'^2}{h^2} \left( 3 + \frac{\kappa^2}{3} \right) \right] \\ & + \frac{f^2}{8\bar{\alpha}^3} \left( -\frac{3h^{(4)}}{h} + \frac{h'h^{(3)}}{h^2} \left( 5 + 6\kappa \coth \kappa - \frac{2\kappa^2}{3} \right) \right. \\ & + \frac{\kappa^4}{15} \left. \right) + \frac{h'^2}{h^2} \left( 1 + 6\kappa \coth \kappa + \frac{\kappa^2}{\sinh^2 \kappa} - \frac{\kappa^2}{3} \right) \\ & - \frac{h^2 h''}{h^3} \left[ 3 + \frac{21}{2} \kappa \coth \kappa + \frac{\kappa^2(92 + 7 \cosh 2\kappa)}{6 \sinh^2 \kappa} \right. \\ & - \frac{\kappa^3(\cosh 3\kappa - 4 \cosh \kappa)}{3 \sinh^3 \kappa} - \frac{7\kappa^4}{45} \left. \right] \\ & + \frac{h'^4}{h^4} \left\{ \frac{5\kappa}{2} \coth \kappa + \frac{\kappa^2}{\sinh^2 \kappa} \left[ \frac{11}{2} + 7\kappa \coth \kappa \right. \right. \\ & - \frac{2\kappa^2}{45} (14 + \cosh 2\kappa) \left. \right] + \frac{4\kappa^2}{3} \left. \right\} + \frac{h'}{945} \left( 2h^4 h^{(5)} \right. \\ & + 8h^3 h' h^{(4)} - 12h^3 h'' h^{(3)} - 27h^2 h'^2 h^{(3)} \\ & - 58h^2 h' h'^2 + 31h h^3 h'' + 44h^5 \left. \right), \quad (A1) \end{aligned}$$

$$\begin{aligned} \gamma'_3(x) = & -\frac{f^6 h'}{8\bar{\alpha}^3 h} + \frac{f^4}{8\bar{\alpha}^3} \left[ \frac{2h^{(3)}}{h} - \frac{h' h''}{h^2} \left( \kappa \coth \kappa + \frac{\kappa^2}{3} \right) \right. \\ & + \frac{h'^3}{h^3} \left( \kappa \coth \kappa - 1 - \kappa^2 \right) \left. \right] + \frac{f^2}{8\bar{\alpha}^3 h} \left\{ -\frac{h^{(5)}}{h} \right. \\ & + \frac{h' h^{(4)}}{h^2} \left( 1 + 2\kappa \coth \kappa + \frac{\kappa^2}{45} \right) + \frac{h'' h^{(3)}}{2h^2} \left( \frac{\kappa^2}{\sinh^2 \kappa} \right. \\ & + 13\kappa \coth \kappa \left. \right) - \frac{h^2 h^{(3)}}{h^3} \left( \frac{5\kappa}{2} \coth \kappa + \frac{15\kappa^2}{2 \sinh^2 \kappa} \right. \\ & - \frac{\kappa^3}{3} \coth \kappa - \frac{\kappa^4}{45} \left. \right) - \frac{h' h'^2}{h^3} \left[ 2\kappa \coth \kappa + \frac{\kappa^2}{2} \right. \\ & + \frac{\kappa^2}{2 \sinh^2 \kappa} (25 + 3\kappa \coth \kappa) - \frac{\kappa^3}{3} \coth \kappa + \frac{\kappa^4}{15} \left. \right] \\ & + \frac{h'^3 h''}{h^4} \left[ \frac{\kappa^2}{2 \sinh^2 \kappa} (11 + 39\kappa \coth \kappa) + \frac{\kappa^3}{6} \coth \kappa \right. \\ & + \frac{\kappa^4}{\sinh^4 \kappa} + \frac{\kappa^2}{2} - \frac{5\kappa^4}{6 \sinh^2 \kappa} - \frac{16}{15} \kappa^4 \left. \right] \\ & + \frac{h'^5}{h^5} \left[ \frac{\kappa^3}{8 \sinh^3 \kappa} (\cosh 3\kappa - 17 \cosh \kappa) - \frac{7\kappa^4}{\sinh^4 \kappa} \right. \\ & - \frac{\kappa^4}{6 \sinh^2 \kappa} (31 - 4\kappa \coth \kappa) - \frac{26\kappa^4}{45} \left. \right] \left. \right\}, \quad (A2) \end{aligned}$$

where  $\kappa = \sqrt{2\bar{\alpha}h(x)}$ . The terms of  $1/D(x)$  independent of  $f$  reproduce its third-order correction for diffusion alone.

Knowing  $D(x)$  and  $\gamma'(x)$  up to certain order enables us to express the stationary 1D density  $p(x)$  from the generalized FJ Eq. (2.10),

$$\frac{p(x)}{h(x)} = \frac{J e^{\gamma(x)}}{(e^{\Delta\gamma} - 1)} \int_{x-L}^x \frac{dx'}{h(x') D(x')} e^{-\gamma(x')}, \quad (A3)$$



respecting periodicity  $p(x) = p(x + L)$ ;  $\Delta\gamma = \gamma(L) - \gamma(0)$ . The net flux  $J$  is obtained from normalization of one particle per period,  $\int_0^L p(x) dx = 1$ . Then the backward mapped 2D density  $\rho(x, y) = \rho_+(x, y) + \rho_-(x, y)$  depicted with colors in Fig. 6 is calculated directly according to the formula (3.2). The components of the corresponding flux density  $\vec{j}(x, y)$ , depicted with the streamlines in Fig. 6, are expressed as

$$\begin{aligned} j_x(x, y) &= -(\partial_x - f)\rho_+ - (\partial_x + f)\rho_- \\ &= [-\partial_x e^{\gamma}(1 + \hat{\omega}) + f e^{\gamma} \hat{\sigma}] e^{-\gamma} \frac{p(x)}{h(x)}, \\ j_y(x, y) &= -\frac{1}{\epsilon} \partial_y \rho = -\frac{1}{\epsilon} e^{\gamma} \partial_y \hat{\omega} e^{-\gamma} \frac{p(x)}{h(x)}. \end{aligned} \quad (\text{A4})$$

The operators  $\hat{\omega}(x, y, \partial_x)$ ,  $\hat{\sigma}(x, y, \partial_x)$  as well as the functions  $\gamma(x)$ ,  $p(x)$  are expressed only up to the order  $\sim \epsilon^3$ , and thus

also the BC (2.2) and the mass conservation,  $\vec{\nabla} \cdot \vec{j} = 0$ , are satisfied only in these orders; hence tiny artifacts may appear in Fig. 6. All analytical calculations and drawings are done in Mathematica.

The numerical solution of the 2D model, given in Fig. 5, was obtained using MATLAB. The procedure was straightforward: discretizing the space by a regular mesh and carefully keeping account of the boundary conditions. The stationary eigenvector of the resulting sparse matrix was then obtained with the built-in MATLAB function `eigs`, which internally implements the Lanczos algorithm. The only subtle point was the extrapolation of the result to an infinitely fine mesh. Indeed, we found that finite lattice spacing in space discretization strongly affects the value of the ratchet current. Therefore, extrapolation to zero lattice spacing is inevitable in order to achieve desired precision.

- 
- [1] P. Reimann, *Phys. Rep.* **361**, 57 (2002).
  - [2] P. Hänggi and F. Marchesoni, *Rev. Mod. Phys.* **81**, 387 (2009).
  - [3] P. Romanczuk, M. Bär, W. Ebeling, B. Lindner, and L. Schimansky-Geier, *Eur. Phys. J. Special Topics* **202**, 1 (2012).
  - [4] E. Fodor and M. C. Marchetti, *Physica A* **504**, 106 (2018).
  - [5] L. F. Valadares, Y.-G. Tao, N. S. Zacharia, V. Kitaev, F. Galembeck, R. Kapral, and G. A. Ozin, *Small* **6**, 565 (2010).
  - [6] A. Walther and A. H. E. Müller, *Chem. Rev.* **113**, 5194 (2013).
  - [7] P. Galajda, J. Keymer, P. Chaikin, and R. Austin, *J. Bacteriology* **189**, 8704 (2007).
  - [8] G. Mahmud, C. J. Campbell, K. J. M. Bishop, Y. A. Komarova, O. Chaga, S. Soh, S. Huda, K. Kandere-Grzybowska, and B. A. Grzybowski, *Nat. Phys.* **5**, 606 (2009).
  - [9] R. Di Leonardo, L. Angelani, D. Dell'Arciprete, G. Ruocco, V. Iebba, S. Schippa, M. P. Conte, F. Mecarini, F. De Angelis, and E. Di Fabrizio, *Proc. Natl. Acad. Sci. USA* **107**, 9541 (2010).
  - [10] A. Sokolov, M. M. Apodaca, B. A. Grzybowski, and I. S. Aranson, *Proc. Natl. Acad. Sci. USA* **107**, 969 (2010).
  - [11] G. Volpe, I. I. Buttinoni, D. Vogt, H.-J. Kümmerer, and C. Bechinger, *Soft Matter* **7**, 8810 (2011).
  - [12] A. Guidobaldi, Y. Jeyaram, I. Berdakin, V. V. Moshchalkov, C. A. Condat, V. I. Marconi, L. Giojalas, and A. V. Silhanek, *Phys. Rev. E* **89**, 032720 (2014).
  - [13] J. E. Sosa-Hernández, M. Santillán, and J. Santana-Solano, *Phys. Rev. E* **95**, 032404 (2017).
  - [14] M. B. Wan, C. J. Olson Reichhardt, Z. Nussinov, and C. Reichhardt, *Phys. Rev. Lett.* **101**, 018102 (2008).
  - [15] I. Berdakin, Y. Jeyaram, V. V. Moshchalkov, L. Venken, S. Dierckx, S. J. Vanderleyden, A. V. Silhanek, C. A. Condat, and V. I. Marconi, *Phys. Rev. E* **87**, 052702 (2013).
  - [16] C. J. Olson Reichhardt and C. Reichhardt, *Annu. Rev. Condens. Matter Phys.* **8**, 51 (2017).
  - [17] R. Alonso-Matilla, B. Chakrabarti, and D. Saintillan, *Phys. Rev. Fluids* **4**, 043101 (2019).
  - [18] P. K. Ghosh, V. R. Misko, F. Marchesoni, and F. Nori, *Phys. Rev. Lett.* **110**, 268301 (2013).
  - [19] P. K. Ghosh, P. Hänggi, F. Marchesoni, and F. Nori, *Phys. Rev. E* **89**, 062115 (2014).
  - [20] B.-Q. Ai, Y.-F. He, and W.-R. Zhong, *J. Chem. Phys.* **141**, 194111 (2014).
  - [21] X. Ao, P. K. Ghosh, Y. Li, G. G. Schmid, P. Hänggi, and F. Marchesoni, *Europhys. Lett.* **109**, 10003 (2015).
  - [22] K. Bisht and R. Marathe, *Phys. Rev. E* **101**, 042409 (2020).
  - [23] M. H. Jacobs, *Diffusion Processes* (Springer, New York, 1967).
  - [24] P. Kalinay and J. K. Percus, *J. Chem. Phys.* **122**, 204701 (2005).
  - [25] P. Kalinay and J. K. Percus, *Phys. Rev. E* **74**, 041203 (2006).
  - [26] S. Martens, G. Schmid, L. Schimansky-Geier, and P. Hänggi, *Phys. Rev. E* **83**, 051135 (2011); *Chaos* **21**, 047518 (2011).
  - [27] P. Kalinay, *Phys. Rev. E* **80**, 031106 (2009).
  - [28] P. Kalinay and J. K. Percus, *Phys. Rev. E* **83**, 031109 (2011).
  - [29] P. Kalinay, *Phys. Rev. E* **84**, 011118 (2011).
  - [30] R. L. Stratonovich, *Radiotekh. Elektron.* **3**, 497 (1958) (in Russian).
  - [31] P. Reimann, C. Van den Broeck, H. Linke, P. Hänggi, J. M. Rubi, and A. Pérez-Madrid, *Phys. Rev. E* **65**, 031104 (2002).
  - [32] S. Lifson and J. L. Jackson, *J. Chem. Phys.* **36**, 2410 (1962).
  - [33] L. Angelani, A. Costanzo, and R. Di Leonardo, *Europhys. Lett.* **96**, 68002 (2011).
  - [34] N. Koumakis, C. Maggi, and R. Di Leonardo, *Soft Matter* **10**, 5695 (2014).
  - [35] A. Pototsky, A. M. Hahn, and H. Stark, *Phys. Rev. E* **87**, 042124 (2013).
  - [36] P. Kalinay, *Phys. Rev. E* **104**, 014608 (2021).
  - [37] M. Sandoval and L. Dagdug, *Phys. Rev. E* **90**, 062711 (2014).
  - [38] E. Yariv and O. Schnitzer, *Phys. Rev. E* **90**, 032115 (2014).
  - [39] P. Malfaretti and H. Stark, *J. Chem. Phys.* **146**, 174901 (2017).
  - [40] R. Zwanzig, *J. Phys. Chem.* **96**, 3926 (1992).
  - [41] D. Reguera and J. M. Rubí, *Phys. Rev. E* **64**, 061106 (2001).
  - [42] M. Kahlen, A. Engel, and C. Van den Broeck, *Phys. Rev. E* **95**, 012144 (2017).
  - [43] E. Aurell and S. Bo, *Phys. Rev. E* **96**, 032140 (2017).
  - [44] P. Kalinay and F. Slanina, *J. Phys.: Condens. Matter* **30**, 244002 (2018).
  - [45] P. Kalinay and F. Slanina, *Phys. Rev. E* **98**, 042141 (2018).